AMERICAN SOCIETY FOR MICROBIOLOGY | Applied and Environmental Microbiology®

MICROBIAL ECOLOGY

Predominance of Anaerobic, Spore-Forming Bacteria in Metabolically Active Microbial Communities from Ancient Siberian Permafrost

Renxing Liang,[a] Maggie Lau,[a]* Tatiana Vishnivetskaya,[b,c] Karen G. Lloyd,[b] Wei Wang,[d] Jessica Wiggins,[d] Jennifer Miller,[d] Susan Pfiffner,[b] Elizaveta M. Rivkina,[c] Tullis C. Onstott[a]

[a]Princeton University, Princeton, New Jersey, USA
[b]University of Tennessee, Knoxville, Tennessee, USA
[c]Institute of Physicochemical and Biological Problems in Soil Science, Russian Academy of Sciences, Pushchino, Moscow Region, Russia
[d]Genomics Core Facility, Princeton University, Princeton, New Jersey, USA

ABSTRACT The prevalence of microbial life in permafrost up to several million years (Ma) old has been well documented. However, the long-term survivability, evolution, and metabolic activity of the entombed microbes over this time span remain underexplored. We integrated aspartic acid (Asp) racemization assays with metagenomic sequencing to characterize the microbial activity, phylogenetic diversity, and metabolic functions of indigenous microbial communities across a ~0.01- to 1.1-Ma chronosequence of continuously frozen permafrost from northeastern Siberia. Although Asp in the older bulk sediments (0.8 to 1.1 Ma) underwent severe racemization relative to that in the youngest sediment (~0.01 Ma), the much lower D-Asp/L-Asp ratio (0.05 to 0.14) in the separated cells from all samples suggested that indigenous microbial communities were viable and metabolically active in ancient permafrost up to 1.1 Ma. The microbial community in the youngest sediment was the most diverse and was dominated by the phyla *Actinobacteria* and *Proteobacteria*. In contrast, microbial diversity decreased dramatically in the older sediments, and anaerobic, spore-forming bacteria within *Firmicutes* became overwhelmingly dominant. In addition to the enrichment of sporulation-related genes, functional genes involved in anaerobic metabolic pathways such as fermentation, sulfate reduction, and methanogenesis were more abundant in the older sediments. Taken together, the predominance of spore-forming bacteria and associated anaerobic metabolism in the older sediments suggest that a subset of the original indigenous microbial community entrapped in the permafrost survived burial over geological time.

IMPORTANCE Understanding the long-term survivability and associated metabolic traits of microorganisms in ancient permafrost frozen millions of years ago provides a unique window into the burial and preservation processes experienced in general by subsurface microorganisms in sedimentary deposits because of permafrost's hydrological isolation and exceptional DNA preservation. We employed aspartic acid racemization modeling and metagenomics to determine which microbial communities were metabolically active in the 1.1-Ma permafrost from northeastern Siberia. The simultaneous sequencing of extracellular and intracellular genomic DNA provided insight into the metabolic potential distinguishing extinct from extant microorganisms under frozen conditions over this time interval. This in-depth metagenomic sequencing advances our understanding of the microbial diversity and metabolic functions of extant microbiomes from early Pleistocene permafrost. Therefore, these findings extend our knowledge of the survivability of microbes in permafrost from 33,000 years to 1.1 Ma.

Citation Liang R, Lau M, Vishnivetskaya T, Lloyd KG, Wang W, Wiggins J, Miller J, Pfiffner S, Rivkina EM, Onstott TC. 2019. Predominance of anaerobic, spore-forming bacteria in metabolically active microbial communities from ancient Siberian permafrost. Appl Environ Microbiol 85:e00560-19. https://doi.org/10.1128/AEM.00560-19.

Editor Alfons J. M. Stams, Wageningen University

Address correspondence to Renxing Liang, rliang@princeton.edu.

* Present address: Maggie Lau, Laboratory of Extraterrestrial Ocean Systems, Institute of Deep-Sea Science and Engineering, Chinese Academy of Sciences, Sanya, Hainan, China.

Received 8 March 2019
Accepted 22 May 2019
Accepted manuscript posted online 31 May 2019
Published 18 July 2019

KEYWORDS aspartic acid racemization, ancient permafrost, microbial activity, spore-forming bacteria

The widely distributed permafrost in the Northern Hemisphere represents an extreme subsurface environment of perpetual subzero temperatures with a limited influx of nutrients sustaining minimal metabolisms in the presence of *in situ* radiation from the decay of U, Th, and K (1, 2). However, the persistence of DNA and a wide diversity and abundance of microbial life have been documented in permafrost deposits in Siberia, Canada, and Alaska (1–3). Previous studies typically targeted total genomic DNA (3–5), which includes intracellular DNA (iDNA) from structurally intact cells (live or dead) and extracellular DNA (eDNA) released through cell lysis or actively excreted from living microbes. Although the ubiquity of eDNA in many habitats, such as soil and marine sediments (6, 7), is acknowledged, the persistence and proportion of eDNA in ancient permafrost remain unknown. Furthermore, recent studies have revealed that the abundant eDNA obscures estimates of microbial diversity in soil (8) and marine sediments (9). Such concerns about relic DNA from necromass might be most relevant for ancient permafrost, because eDNA is better preserved at subzero temperatures (10). In this regard, it is important to sequence the iDNA and eDNA fractions in order to determine whether the phylogenetic diversity and function of these two DNA fractions are distinct and, if so, whether they record extant versus extinct microbial communities in ancient permafrost.

The mechanisms for the long-term survival strategies of cold-adapted microorganisms in ancient permafrost have been investigated in several studies (3, 11–14). Given the harsh conditions in ancient permafrost, microbial dormancy is considered to be a major mechanism to maintain long-term viability over geological time (15). Many spore-forming bacteria within the classes *Clostridia* and *Bacilli* have been cultivated frequently from ancient permafrost in Siberia (16–19), Canada (20), and northern Norway (21). Moreover, a recent metagenomic study revealed that the relative abundance of spore-forming bacteria increased from 13% to 79% along a 19,000- to 33,000-year (19- to 33-kyr) chronosequence in Alaskan permafrost (3). In older permafrost sediments of 400 to 600 kyr, two studies have found that non-spore-forming *Actinobacteria* were more dominant than the spore-forming *Firmicutes* (10, 13). These observations that spore-forming bacteria are more dominant than non-spore-forming *Actinobacteria* in 5- to 33-kyr permafrost but that *Actinobacteria* are more dominant than spore-forming bacteria in much older permafrost might be reasonably justified because spores are not metabolically active (22). Therefore, metabolic activity and DNA repair of non-spore-forming bacteria may be essential for survival in permafrost $>$50 to 200 kyr old (13, 23, 24). Although non-spore-forming bacteria, such as *Actinobacteria*, were more frequently isolated from Siberian permafrost sediments ranging in age from 10 kyr to 3 million years (3 Ma), the cultivation of spore formers capable of growth at subzero temperatures has been reported from 3-Ma-old permafrost (16–19). It has been hypothesized previously that the spore formers in ancient permafrost might be present as active vegetative cells instead of being in a dormant state (14).

Aspartic acid (Asp) racemization measurements and modeling have been utilized to constrain microbial anabolic activity, thereby constraining the relative amounts of active versus dormant cells in marine sediments, deep subsurface fracture water, and permafrost sediments (25–30). The Asp racemization model has been shown to work well in subsurface permafrost sediments with known, stable temperature records and established geological ages (25, 31). According to the D-Asp/L-Asp ratio of bulk sediments, these studies (25, 31) concluded that the microbes should be metabolically active in ancient permafrost up to 25 kyr old. However, the D-Asp/L-Asp ratios measured from the bulk sediments of greater ages (25 to 40 kyr) were too high to allow the claim that the microbial activity level was higher than that required for protein maintenance (31). Since the active vegetative cells might contribute to only a small fraction of the total Asp in the frozen sediments, the D-Asp/L-Asp ratio in cells detached from sedi-

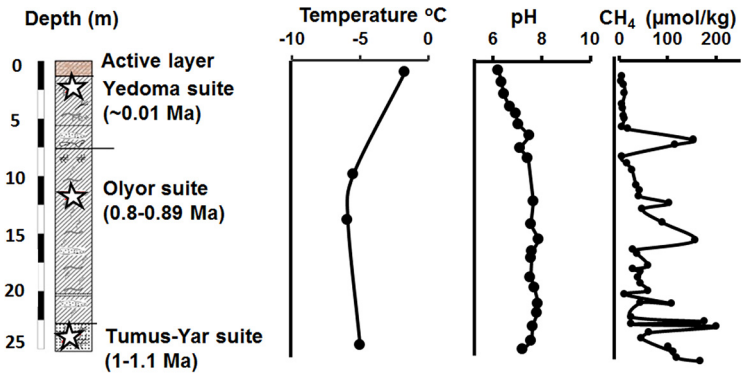

FIG 1 Diagram of core sediment (0.0 to 25.05 m) from borehole AL1-15. The temperatures, pHs, and concentrations of CH_4 at various depths are shown to the right of the diagram. Stars indicate the depths of samples (1.4, 11.8, and 24.8 m) that were selected for Asp racemization and DNA extraction for microbial community characterization.

ments would provide a more accurate estimate of the microbial activity in ancient frozen permafrost (31).

The geological ages of the permafrost sediments in the Kolyma-Indigirka Lowland of Siberia span a long chronosequence, from the Holocene to the Pliocene era, over a depth of 600 to 800 m (32, 33). The layers of permafrost sediments harbor various types of organisms that were buried thousands to millions of years ago (31, 34). In this study, frozen sediments ranging in age from 0.01 to 1.1 Ma were selected to provide a unique window into the selective survivability and microbial activity of soil microbial communities progressively buried and isolated in permafrost through geological time under the assumption that the soil microbial communities originally present in the 1.1-Ma active layer before burial and freezing are very similar to those present in the 10-kyr active layer before burial and freezing (10). The phylogenetic diversity and metabolic potential of the indigenous microbial communities were interrogated with 16S rRNA amplicon and shotgun metagenomic sequencing of the eDNA and iDNA pools. Additionally, to shed light on the metabolic status and mechanisms for long-term survival of the *in situ* microflora, we measured the D-Asp/L-Asp ratios in the bulk sediment samples and the separated cells. Our results suggest that the 10-kyr–to–1.1-Ma permafrost chronosequence records the selection of a microbial community dominated by anaerobic, spore-forming bacteria within the *Firmicutes* that have remained metabolically active during freezing, burial, and isolation over geological time from a more-diverse active-layer microbial community dominated by *Actinobacteria* and *Proteobacteria*, which have mostly died off.

RESULTS AND DISCUSSION

Geochemical characteristics. The *in situ* temperature ranged from −2 to −6°C at a 1- to 25-m depth in the borehole (Fig. 1). These temperatures were higher than the mean annual temperatures of wells (−11 to −13°C) drilled in the Kolyma Lowland area in 2002 (25). The pH was slightly acidic (6.22 to 6.93) in the upper layers (0.8 to 4.6 m), whereas the deeper strata exhibited more neutral pHs, ranging from 7.03 to 7.88 (Fig. 1). The concentrations of methane in the core sediment differed greatly, from 4 to 200 μmol/kg, at various intervals (Fig. 1). The detection of ancient methane and methanogenic activity in Siberian permafrost has been reported frequently in previous studies (33, 35). The concentrations of the major anions (Cl^-, SO_4^{2-}, NO_2^-, and NO_3^-) in the water extracts from the three depths sampled (1.4, 11.8, and 24.8 m) were generally $<$10 μg/g, with slight variations (see Table S2 in the supplemental material). As reported in a previous study (32), the presence of various electron acceptors could be utilized by indigenous microorganisms to drive denitrification and sulfate reduction at this particular site.

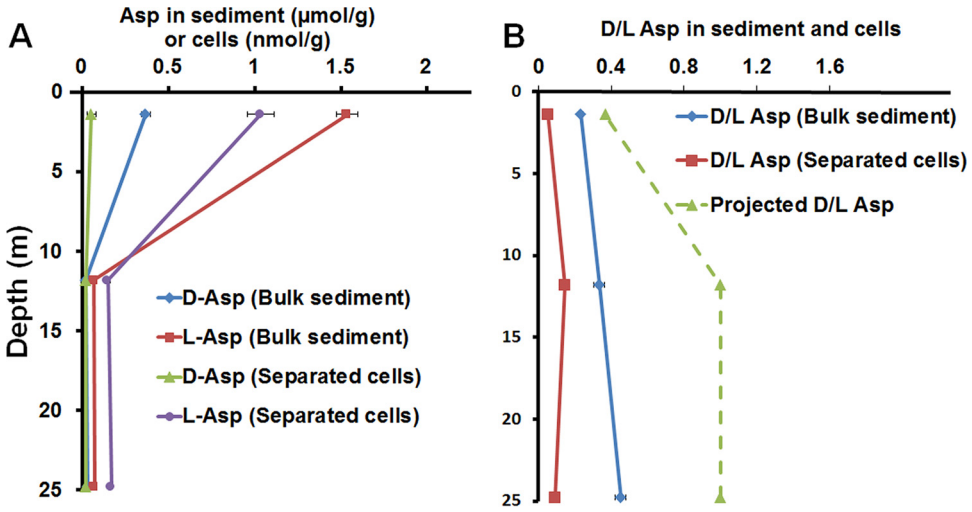

FIG 2 (A) Concentrations of D-Asp and L-Asp in bulk sediment and separated cells. (B) D-Asp/L-Asp ratios in bulk sediment and separated cells and projected D-Asp/L-Asp ratio according to the Asp racemization model using the geological age of permafrost.

Asp racemization in bulk sediments. The concentration of L-Asp in the youngest layer (1.54 ± 0.06 μmol/g) was approximately 22 times higher than that in the older sediments (0.07 ± 0.01 μmol/g) (Fig. 2A). D-Asp was also detected (up to 0.37 ± 0.03 μmol/g at 1.4 m), and the concentration showed a decreasing trend with depth similar to that of L-Asp (Fig. 2A). Interestingly, the D-Asp/L-Asp ratio in the bulk sediment increased with geological age (Fig. 2B). The increase in D-Asp/L-Asp ratios with geological age has been shown previously in Siberian permafrost up to 0.04 Ma old (25, 31) and in subseafloor sediments up to several million years old (26, 28, 29, 36). Therefore, our results confirmed that Asp in buried sediment was subjected to racemization through geological time even at subzero temperatures in frozen permafrost. Since temperature is a major factor influencing racemization, the racemization rate of Asp has been extrapolated to a subzero temperature (−4°C) in marine sediment based on heating experiments in a previous study (37). If the initial D-Asp/L-Asp ratio in the bulk sediment before freezing is assumed to be zero, then the Asp racemization in the older sediments would achieve equilibrium with a D-Asp/L-Asp ratio of 1 (Fig. 2B). Obviously, the actual D-Asp/L-Asp ratio was much lower than 1 (Fig. 2), suggesting that the microbial cells in the deeper, older permafrost were sufficiently metabolically active to maintain a low D-Asp/L-Asp ratio, but calculation of an *in situ* metabolic rate would require further amino acid analyses and assumptions regarding the metabolic yields and protein repair processes of the active microorganisms (27).

Cell separation and cellular D-Asp/L-Asp ratio. Since D-Asp and L-Asp in the bulk sediments originated from total biomass and necromass present in the sediments, it is critical to separate cells from sediments and to determine the cellular D-Asp/L-Asp ratio in ancient permafrost. Both green and red fluorescently stained cells of different morphologies and sizes were observed in all samples (see Fig. S2 in the supplemental material). The total cell counts decreased dramatically with depth and age (Fig. S2 and S3), a finding consistent with fluorescently stained cell counts in marine (26, 28) and lake (38, 39) sediments. Notably, the percentage of potentially viable cells (22.8%) at 1.4 m was similar to those in coastal marine sediments (40) and in permafrost from Alaska (3) and northern Norway (21). It should be noted that membrane-compromised cells are not necessarily dead and that membrane integrity does not guarantee microbial activity (40), particularly in ancient permafrost with numerous stressors.

In accord with the observed trend in the bulk sediment (Fig. 2A), the concentration of Asp in separated cells from the youngest sample (1.03 ± 0.08 nmol/g) was much higher than that from the deeper and older sediments at 11.8 and 24.8 m (0.15 ± 0.01

and 0.17 ± 0.01 nmol/g, respectively). However, the cellular Asp content accounted for only a small fraction (~0.05 to 0.2%) of the total Asp in the bulk sediment. Interestingly, the D-Asp/L-Asp ratio in the cells (0.05 to 0.14) was much lower than that in the bulk sediment at each depth (Fig. 2B). This range overlaps the D-Asp/L-Asp ratios of different bacterial species (0.02 to 0.12) (27, 29). Furthermore, the D-Asp/L-Asp ratios in cells extracted from subseafloor sediment and deep fracture fluids were 0.014 to 0.085 (41) and 0.037 to 0.095 (27), respectively. Therefore, the D-Asp/L-Asp ratios from separated cells in ancient permafrost were similar to those determined from live pure cultures and the active microfloras in different subsurface environments. More importantly, the actual D-Asp/L-Asp ratios in separated cells were much less than the D-Asp/L-Asp ratio predicted due to purely chemical racemization at all depths (Fig. 2B). Taking these findings together with the evidence from live-cell staining (Fig. S2 and S3 in the supplemental material), we conclude that the extant microbial communities are viable and are sufficiently metabolically active to maintain a relatively low D-Asp/L-Asp ratio at subzero temperatures in ancient permafrost up to 1.1 Ma old.

Microbial diversity. Previous studies showed that amplifiable DNA products were detected only in permafrost samples younger than 400 to 600 kyr due to severe DNA damage (10, 13). In our study, detectable and amplifiable DNA was obtained in much older permafrost, as old as 1.1 Ma (see Table S3 in the supplemental material). The decreasing trend for total-DNA yield (Table S3) with geological age was consistent with previous reports on ancient permafrost samples up to 400 to 600 kyr old (10, 13). Alpha diversity (Chao1 and Shannon indices) decreased dramatically with age (see Fig. S4 in the supplemental material), an observation consistent with previous findings in ancient permafrost in Siberia (10, 13) and Alaska (3). Principal-coordinate analysis (PCoA) revealed that microbial communities determined from iDNA and eDNA fractions were significantly different ($P < 0.001$) from one another (see Fig. S5). Permutational multivariate analysis of variance revealed that the variation in beta diversity among iDNA fractions could be largely explained by depth (42%; $F = 2.9$; $P < 0.05$) and age (51%; $F = 4.1$; $P < 0.01$). That depth and age were found to be the primary determinants probably reflects the depletion of nutrients and the long-term exposure to cold temperatures and highly reduced conditions in the deeper/older sediments through geological time. The eDNAs of the 11.8-m and 24.8-m samples, however, clustered close to that of the blank controls, as shown by weighed UniFrac PCoA analysis (Fig. S5B). Therefore, many operational taxonomic units (OTUs) in the eDNA fractions at 11.8 and 24.8 m originated from the common contaminants from reagents and the laboratory environment (42) and do not reflect environmental parameters.

As revealed by 16S rRNA amplicon and metagenomic sequencing of iDNA fractions (Fig. 3; see also Fig. S6 in the supplemental material), the relative abundances of *Actinobacteria*, *Acidobacteria*, and *Chloroflexi* decreased with geological age. The phylum *Firmicutes* was overwhelmingly predominant in iDNA fractions from the older sediments at 11.8 and 24.8 m (Fig. 3; also Fig. S6). Despite the difference in relative abundances between 11.8 and 24.8 m, most of these microbial lineages were identified as belonging to the class *Clostridia* (Fig. S6 and S7), which is typically composed of anaerobic, spore-forming bacteria. Although the majority of the OTUs (35.8 to 87.2%) were present exclusively in the iDNA fractions (Fig. 4), 267 OTUs are shared among all the iDNA fractions (see Fig. S8). The shared community was composed mainly of the phyla *Firmicutes*, *Actinobacteria*, *Proteobacteria*, and *Chloroflexi* (Fig. S8). These microbial lineages commonly found in soil are apparently persistent in permafrost irrespective of geological age. More interestingly, 44.5% (1,293) of the total OTUs in the iDNA of the 11.8-m sample were shared with the iDNA of the 1.4-m sample, whereas only 10.5% of the total number of OTUs in the iDNA of the 11.8-m sample were shared with the iDNA of the 24.8-m sample (Fig. S8). Overlapping OTUs between the young and old permafrost sediments have been reported previously (10), suggesting that the original microflora present in the deepest older sediments share some similarity with the microbial community in the youngest, shallowest

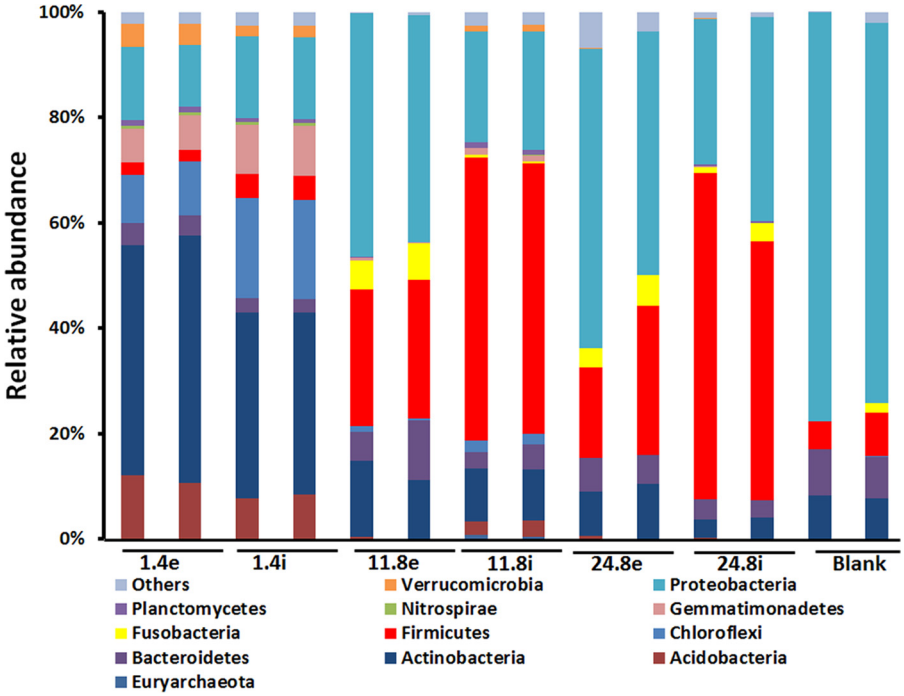

FIG 3 Comparison of microbial community compositions at the phylum level determined by 16S rRNA amplicon sequencing. Only major phyla representing >1% of the whole microbial community are shown for bacteria. Note that two replicates were analyzed in each sample.

permafrost layer. These shared OTUs provide an opportunity to examine species-level changes over the course of depositional time and as a function of increasing subsurface isolation time upon freezing. Recovery of draft genomes of these ancient and modern microbial species with deeper sequencing would provide further

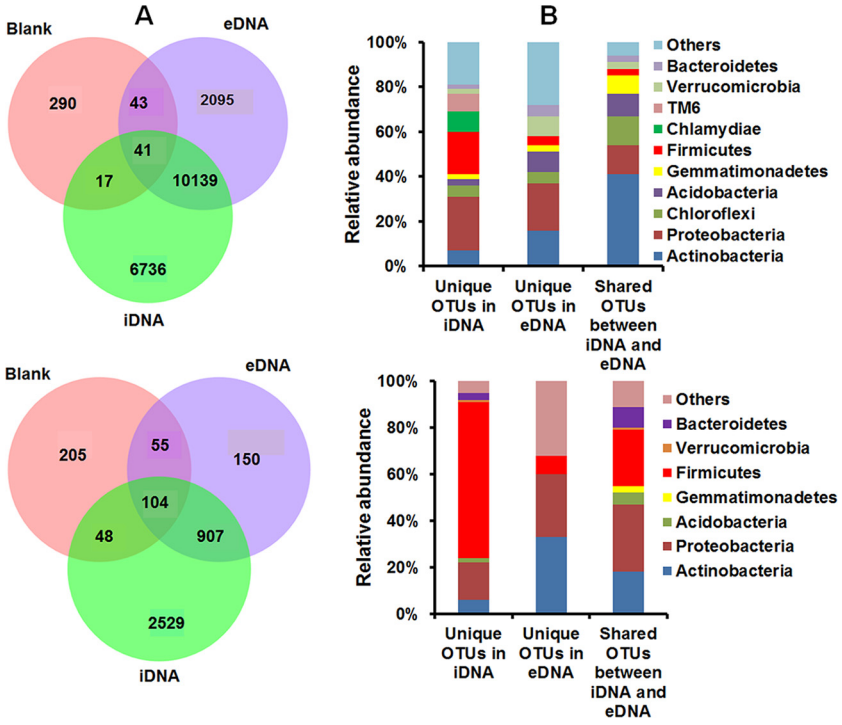

FIG 4 Venn diagrams of OTUs from eDNA, iDNA, and extraction blanks (A) and taxonomic distributions in iDNA, eDNA, and shared OTUs (B) from sediments at 1.4 m (top) and 11.8 m (bottom).

information about the mechanism of long-term evolution in cryogenic environments throughout geological time.

The eDNA fractions represent a mixture of nucleic acids excreted from the extant microbial communities and lysed microbial cells. In the youngest permafrost sediment, the number of OTUs unique to the 16S rRNA gene amplicons of the eDNA fraction was 2,095; these likely represent lysed microbial cells, whereas 10,139 OTUs were shared with the iDNA fraction and might represent 16S rRNA genes of recently lysed microbial cells or an artifact from the DNA extraction process (Fig. 4). In the deep, older sediments, however, most of the OTUs in the iDNA fractions were unique (~70 to 90%), and a much smaller proportion of the eDNA pool was unique: only 150 OTUs in the case of the 11.8-m sample. This suggests that little of the DNA from lysed cells (unique OTUs in the eDNA) survives for 1.1 Ma in a frozen state. However, caution should be exercised, because the absence of OTUs in either the eDNA or the iDNA fraction could also be attributed to the detection limit of the approach employed in this study. The spore-forming bacteria within *Firmicutes* were predominant among the unique OTUs of the iDNA pools, whereas *Actinobacteria* and *Proteobacteria* were more abundant in unique OTUs from eDNA fractions (Fig. 4; see also Fig. S9 in the supplemental material). Such differences between the inferred physiology of the ancient relic DNA (unique OTUs in the eDNA) and that of the iDNA suggest that most aerobes became extinct, whereas the spore-forming bacteria affiliated with the phylum *Firmicutes* survived the ~1 million years of entrapment in the ancient permafrost.

In comparison, the percentage of overlapping OTUs between the iDNA and eDNA fractions in the coastal soil of the Atacama Desert of Chile was 88%, and that in the hyperarid core soils of the Atacama Desert was 20% (43). Since a portion of the 16S rRNA gene of the eDNA pool can be continually replenished by turnover of microbial biomass (44), Schulze-Makuch et al. (43) argued that the microbial activity in coastal soil was much higher than that of the hyperarid core due to greater humidity and nutrient abundance. The overlap in OTUs from our results ranged from 53% for the youngest permafrost to 6 to 25% for the oldest permafrost (Fig. 4; also Fig. S9 in the supplemental material), suggesting that, as in the Atacama Desert, the microbial activity in the youngest permafrost sediment was likely much higher than that in the older permafrost sediments due to the higher temperature (Fig. 1) and availability of labile organic matter in the Yedoma deposits (45).

Predominance of anaerobic metabolisms in the deeper sediments. The subsequent functional analyses of the five metagenomes provided further evidence that the potential metabolic pathways of the microbial communities became predominantly anaerobic in the deeper, older strata (11.8 and 24.8 m), in contrast to the youngest layer, which was enriched with genes related to aerobic metabolism. For example, genes encoding various types of cytochrome oxidases were enriched (Fig. 5A) only in the Holocene sediment from the Yedoma suite (Fig. 1). Genes encoding high-O_2-affinity terminal oxidases (microaerobic; the combination of cbb_3 and *bd* types) were collectively more abundant than low-O_2-affinity terminal oxidases (aerobic; aa_3 type), suggesting that microaerobic metabolism dominates in the top Yedoma permafrost layer (Fig. 1). Genes linked to the aerobic oxidation of methane (the particulate methane monooxygenase gene [*pmoA*]), ammonia (the ammonia monooxygenase [*amoA*] and hydroxylamine oxidoreductase [*hao*] genes), and methanol (the methanol dehydrogenase gene [*mxaF*]) were detected only in the 1.4-m sample. Genes associated with the denitrification pathway (the *napA*, *nirK*, and *nosZ* genes) were enriched in the 1.4-m sample relative to the deeper samples (Fig. 5A). In contrast, functional genes linked to anaerobic metabolism processes, such as dissimilatory sulfate reduction (dissimilatory sulfite reductase [encoded by *dsrA* and *dsrB*]), methanogenesis (α-subunit of methyl-coenzyme M reductase [encoded by *mcrA*]), and H_2 production (Fe-Fe hydrogenase), were more abundant in the deeper sediments, particularly at 24.8 m (Fig. 5A). The potential for anaerobic metabolism deduced from the metagenomic data suggests that highly reduced, anoxic conditions were created in the deeper frozen sediment to

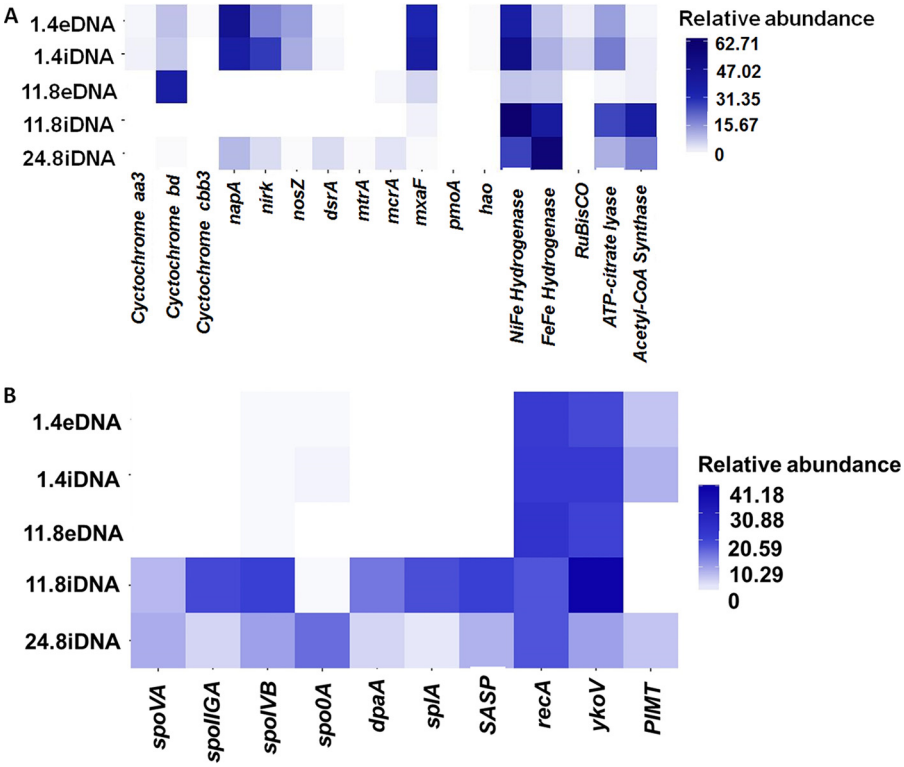

FIG 5 Relative abundances of functional genes related to metabolism with different electron acceptors (A) and genes associated with long-term survival mechanisms, including sporulation and DNA repair (B).

support anaerobic microbial respiration with various electron acceptors (32). For the youngest, shallowest permafrost sediment, where cell turnover appears to have been the greatest, the metagenomic data suggest that either a microaerophilic environment was captured at the time of freezing or the diffusion of O_2 from the overlying active layer through patchy epigenetic pore ice is sustaining microaerophilic respiration today.

Long-term survival strategies in Pleistocene permafrost. A suite of sporulation-related genes was found to be highly enriched in the metagenomes of the deeper samples relative to their abundances in the metagenome of the youngest permafrost sediment (Fig. 5B), which is not surprising given the predominance of anaerobic, spore-forming bacteria (mostly *Clostridia*) in the deeper, older layers (Fig. 3). Among these genes, *spo0A*, *spoIIGA*, and *spoIVB* are involved in various stages of sporulation (46, 47). The *dpaA* and *spoVA* genes are involved in the synthesis and transport of dipicolinic acid (DPA) (48), whereas SASP genes encode *s*mall, *a*cid-*s*oluble *p*roteins (SASPs) in spores (49). The high level of DPA in spores and the complexation of DNA by SASPs are important for the long-term survival of spores (22). Notably, the gene encoding spore photoproduct lyase (*splA*), which is known for the repair of DNA damage caused by UV radiation (50), was also enriched in the deeper samples. Additionally, other genes (*recA* and *ykoV*) that are potentially important in DNA repair (51, 52) were detected at high abundances from all samples (Fig. 5B). Intriguingly, the gene encoding the protein repair enzyme PIMT (protein L-isoaspartyl/D-aspartyl *O*-methyltransferase) was present at low abundances at all depths (Fig. 5B). Therefore, PIMT is a plausible means through which the low cellular D-Asp/L-Asp ratio (Fig. 2B) was maintained, by converting isomerized Asp (iso-Asp) or racemized Asp (D-Asp) back to L-Asp residues in metabolically active microbial cells (53). Since PIMT is found only in Gram-negative bacteria and archaea (54), the dominant Gram-positive spore-forming bacteria from the older permafrost are either replacing their enzymes deactivated by

Asp racemization or repairing their damaged proteins by an unknown mechanism. Both processes require metabolic activity, though the latter requires less than the former.

The overwhelmingly predominant spore-forming bacteria (Fig. 4) and the enrichment of sporulation-related genes (Fig. 5B) in the iDNA fraction of older sediments (0.8 to 1.1 Ma) indicate that microbial dormancy might play a critical role in long-term survival under frozen conditions. The increase in spore-forming bacteria in older permafrost was broadly similar to that observed in a recent study of Alaskan permafrost up to 33 kyr in age (3) but contradicts other studies from Siberia permafrost up to 400 to 600 kyr (10, 13). The greater abundance of non-spore-forming bacteria (*Actinobacteria*) than of spore formers (*Firmicutes*) in these older permafrost samples was ascribed to the metabolic activity and DNA repair of non-spore-forming bacteria (13, 24). Due to the lack of high-energy compounds in dormant endospores (55), microorganisms buried in ancient permafrost must maintain low levels of metabolic activity to repair DNA and protein damage in order to survive through geological time. Therefore, the predominant spore-forming bacteria in the older permafrost of this study should be in an active metabolic state instead of dormancy (14). This postulation was corroborated by several lines of evidence, including the low cellular D-Asp/L-Asp ratio (Fig. 2B), live-cell staining (Fig. S2 and Fig. S3 in the supplemental material), and the predominance of spore-forming bacteria in iDNA pools from the older permafrost (Fig. 4; also Fig. S6 and S7). Due to limited nutrient influx in the sealed, frozen systems, it is possible that the dominant spore-forming bacteria survived as persisters that can maintain minimum activity to repair DNA and proteins over prolonged periods (14).

Microbial interactions involved in the metabolism of ancient carbon. Ancient permafrost represents a large reservoir of organic carbon that can be utilized by the indigenous microbial community (2, 56). Not surprisingly, genes involved in the degradation of different carbon compounds were detected at all depths with various abundances (Fig. 6A). The relative abundances of genes for the hydrolysis of labile sugars, such as starch (amylase) and sucrose (sucrase), were much higher in the youngest sediment (Fig. 6A). In contrast, the genes responsible for the degradation of recalcitrant carbon (xylosidase and galactosidase) were more abundant in the deeper, older sediments (Fig. 6A). The enrichment of genes involved in utilizing various carbohydrates has also been reported in 19- to 33-kyr-old Alaskan permafrost (3). Apart from the fermentation of carbohydrates, numerous proteolytic enzymes from the cysteine peptidase, metallopeptidase, and serine peptidase families (57) were detected in all three permafrost samples (Fig. 6B). However, peptidases from anaerobic protein-degrading microorganisms (clostripain, papain, and pyroglutamyl peptidase) (58) were more numerically abundant in the older strata. Furthermore, the key genes involved in the intracellular biodegradation of amino acids were highly enriched in the deeper, older sediment relative to the youngest layer (Fig. 6B). For instance, the ferredoxin-reducing oxidoreductase specific for aldehydes (AOR), 2-ketoisovalerate ferredoxin oxidoreductase (VOR), and indolepyruvate ferredoxin oxidoreductase (IOR) were more abundant in the older sediment (Fig. 6B). These ferredoxin-reducing oxidoreductases are highly O_2 sensitive (59) and are known to be involved in the breakdown of both nonaromatic and aromatic amino acids in *Clostridium* species (60). Therefore, the dominant bacteria associated with *Clostridia* in the deep, ancient permafrost have the genetic potential to cycle detrital proteins and further ferment amino acids throughout geological time.

Due to the fermentative capabilities of the predominant spore-forming *Clostridia*, genes involved in the production of formate (pyruvate formate lyase), acetate (acetate kinase), and butyrate (butanol dehydrogenase and butyrate kinase) were more numerically abundant in the older sediments (Fig. 6B). These fatty acids generated from fermentative processes can be utilized by the sulfate-reducing bacteria and syntrophic bacteria detected in the older permafrost sediments. For example, the most dominant sulfate-reducing bacteria, *Desulfosporosinus* species, are able to oxidize short-chain fatty acids (e.g., acetate, propionate, and butyrate) with sulfate, nitrate, and Fe(III) as electron

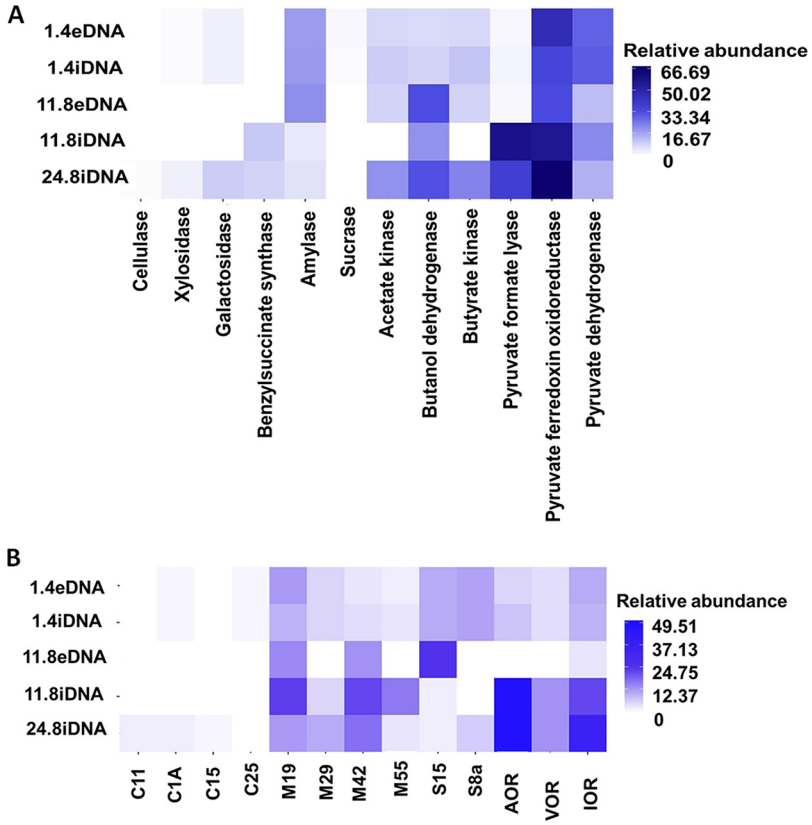

FIG 6 Relative abundances of functional genes related to carbohydrates (A) and the fermentation of peptides and amino acids (B). C, cysteine peptidases; M, metallopeptidases; S, serine peptidases.

acceptors (61, 62). Additionally, several syntrophic bacteria from the genera *Syntrophomonas* and *Smithella* were detected in the older permafrost. These microbial lineages are well known for their ability to syntrophically oxidize fatty acids when coupled with hydrogenotrophic methanogens (63, 64). Notably, small fractions (<1%) of hydrogenotrophic methanogens (mainly *Methanoregula* species) were detected in the iDNA fractions from the older strata. The *mcrA* sequences from the older sediments showed the highest similarity to *Methanoregula formicica* SMSP^T, an isolate from methanogenic sludge (65), and *Methanoregula boonei* 6A8, isolated from an acidic peat bog (66). Furthermore, the key enzyme acetyl coenzyme A (CoA) synthase, involved in autotrophic CO_2 fixation (Wood-Ljungdahl pathway), was highly enriched in the older permafrost relative to its abundance in the youngest permafrost. The presence of acetyl-CoA synthase and its role in anabolic CO_2 fixation have been reported in the genomes of *Methanoregula formicica* SMSP^T (65) and *Methanoregula boonei* 6A8 (66). Since various amounts of CH_4 were indeed detected at different depths of the borehole (Fig. 1) with $\delta^{13}C$ values of −85‰ VPDB (67), the archaeal lineages from the genus *Methanoregula* identified in the older sediments might contribute to methane production by utilizing CO_2 and H_2 in the sealed, frozen ecosystem with limited nutrient flux.

Conclusions. The ubiquity of relic DNA in many habitats, including water, soil, and sediment, has raised some concerns about its impact on microbial community diversity estimates (8, 9, 68). We simultaneously extracted the DNA from intact cells (iDNA) and the extracellular DNA (eDNA), potentially representing past, relic microbial lineages preserved in a 0.01- to 1.1-Ma chronosequence of permanently frozen sediments. The OTUs in the eDNA that are not shared with those of the iDNA pools suggested that certain ancient species became extinct (i.e., not members of metabolically active subsurface permafrost communities), whereas other microorganisms represented by OTUs in the iDNA pool remained active through geological time. The overlapping core

community among iDNA pools from all samples (see Fig. S8 in the supplemental material) indicated that a subset of microorganisms in the older layers were also present in the youngest permafrost in the Yedoma deposits. The predominance of anaerobic, spore-forming bacteria in the iDNA fractions from the older permafrost suggested that microbial dormancy might have played important roles in maintaining survivability over prolonged periods of geological time. Due to the lack of metabolic activity in dormant spores, the predominant spore-forming bacteria might be present as active, vegetative cells instead of dormant forms in order to maintain the observed low cellular D-Asp/L-Asp ratio. Indeed, live-cell staining and the Asp racemization assay of the separated cells indicated that many indigenous microorganisms buried in the oldest permafrost in the Northern Hemisphere may represent living microbial communities that are metabolically active. Due to the low DNA yield and limited sequencing depth, no metagenome-assembled genomes (MAGs) could be recovered to further elucidate the adaptation and evolution mechanisms of the surviving microbial populations in the ancient permafrost. With a combination of metagenomics and single-cell-amplified genomes (SAGs), a previous study has revealed that the evolutionary changes of microbial genomes were undetectable in subsurface marine sediments thousands of years old (69). Therefore, in the future, studies to recover MAGs or SAGs should be pursued in order to confirm whether the surviving species have undergone adaptive evolution in frozen sediments that are millions of years old.

MATERIALS AND METHODS

Sample collection from ancient permafrost sediment. The sampling site was located within the Kolyma–Indigirka Lowland in northeastern Siberia (see Fig. S1 in the supplemental material). Borehole AL1-15 (69°20.44′N, 154°59.71′E; elevation, 13 m) was drilled on the floodplain close to the Alazeya River (Fig. S1) in August 2015. The drilling operations and the aseptic techniques employed to prevent contamination have been described previously (17, 35). Permafrost cores were extracted using drilling equipment that operates without drilling fluids. This drilling method prevents downhole contamination and reduces the environmental impact. Extracted cores were processed inside a field laboratory tent. The surfaces of 20- to 30-cm-long cores were cleaned by removing melted layers with an ethyl alcohol-sterilized knife, and the frozen internal parts of the cores were placed in sterile Whirl-Pak bags and were kept frozen at −15°C in a Dometic CFX 50W powered cooler during storage in the field and transportation. The downhole *in situ* temperature was measured immediately after coring had been completed. Permafrost sediments were collected from various intervals of the core for geochemical characterization. Three samples (1.4, 11.8, and 24.8 m below the surface) of permafrost sediments were selected for geochemical, aspartic acid, and DNA analyses (Fig. 1), transported on dry ice to Princeton University, and stored at −80°C until analyses.

Permafrost can form syngenetically, where freezing occurs during sediment deposition and burial, or epigenetically, where freezing occurs long after deposition (33). The youngest permafrost, sampled at a 1.4-m depth, was silty loam of the Yedoma suite, which was syngenetically frozen ~0.04 Ma ago. However, the age of permafrost at 1.4 m is ~0.01 Ma, late Pleistocene to early Holocene, younger than the Yedoma deposits, because the frozen sediment was thawed and refrozen at this location, as indicated by the absence of large ice wedges (70). According to the stratification record (17, 56), the sediments at 11.8 m and 24.8 m were from the formations of the Olyor (0.8 to 1.6 Ma) and Tumus-Yar (1.8 to 2.2 Ma) suites, respectively. Since the permafrost at these depths was formed epigenetically, the permafrost ages at 11.8 m and 24.8 m were estimated to be ~0.8 to 0.89 Ma and ~1 to 1.1 Ma (early Pleistocene), respectively.

Porewater chemistry. Anion samples were derived from porewater extracts of the internal cores, and concentrations of fluoride, chloride, bromide, nitrite, nitrate, sulfate, phosphate, formate, acetate, and propionate were measured by an ion chromatograph (Dionex IC25) coupled to an electrospray ionization (ESI)-quadrupole mass spectrometer (MSQ; Thermo Scientific, USA).

DNA extraction and 16S rRNA amplicon sequencing. To simultaneously extract eDNA and iDNA from permafrost sediments, a procedure suitable for large-scale extraction was modified from a previous study (71). Since the biomass in the ancient permafrost is typically low (2), large quantities of materials (10 to 40 g) were used to extract iDNA and eDNA with a DNeasy PowerMax soil kit (Qiagen, Carlsbad, CA). Phosphate buffer (0.12 M Na_2HPO_4 [pH 8]) was filter sterilized through a 0.2-μm-pore-size membrane before being used for eDNA extraction. Each 10-g permafrost sediment sample was thawed and mixed with 8.1 ml of phosphate buffer. After shaking at 300 rpm for 15 min, the slurry was centrifuged at 10,000 × *g* for 10 min at 4°C. The supernatant was transferred to a new 50-ml Falcon tube without disturbing the sediment, and another 8.1 ml of phosphate buffer was added to the remaining sediment. The same procedure for mixing the slurry was repeated, and the supernatant was removed after centrifugation. The combined supernatant (~16.2 ml) containing eDNA was extracted by following the manufacturer's procedures with the extraction kit except that the steps for bead beating and cell lysis were bypassed. The sediment remaining after eDNA removal was used to extract iDNA according to the standard protocol of the same extraction kit. Sediment-free blank controls for eDNA and iDNA were

subjected to the respective procedures as described above in order to track potential contamination introduced from the reagents and laboratory environment during extraction. The concentration of DNA was quantified using a Qubit 3.0 fluorometer with the dsDNA HS assay kit (Invitrogen, Carlsbad, CA, USA). Since the DNA yield from 24.8 m was below the Qubit detection limit (0.01 ng/μl), a total of four 10-g samples were used for extraction, and the final DNA products were combined for subsequent analyses.

For the preparation of the library for 16S rRNA amplicon sequencing, a dual-indexed PCR amplification strategy was used to amplify the 16S rRNA gene V4 region with a universal primer set targeting most bacteria and archaea (515F/806R) (72). PCRs were prepared in a 25-μl (final volume) reaction mixture containing KAPA HiFi HotStart ReadyMix (12.5 μl), primers (final concentration, 2.5 μM), and 1 to 5 μl DNA template depending on the DNA concentration. The PCRs consisted of initial denaturation at 94°C for 3 min; 25 or 30 cycles of denaturation at 94°C for 45 s, annealing at 50°C for 1 min, and extension at 72°C for 10 min; and a final extension step at 72°C for 10 min. The DNAs extracted from sediment-free blank controls were also amplified. All amplicon products were pooled at equal molar ratios and were sequenced on an Illumina HiSeq 2500 system (150 bp, paired end) in the Genomics Core Facility at Princeton University. The dual-indexed samples were demultiplexed, and the raw reads were quality-filtered (Phred score, $\geq$30) using Galaxy pipelines at Princeton University. The trimmed sequences were further analyzed by QIIME (Quantitative Insights Into Microbial Ecology) (73) using the Silva database, release 128 (74). Chimeric sequences were removed, and operational taxonomic units (OTUs) were clustered using a 97% similarity threshold. The alpha-diversity metrics (Chao1 and Shannon indices) were calculated and visualized using the Web-based tool MicrobiomeAnalyst (75). Statistical differences in alpha diversity between groups of samples were computed using one-way analysis of variance (ANOVA) in MicrobiomeAnalyst. Beta diversity was computed using weighted and unweighted UniFrac distances, and then PCoA were performed to visualize the relationship and clustering among samples. Permutational multivariate ANOVA (Adonis function in QIIME) was used to assess correlations between community composition and metadata such as geological age, depth, and physiochemical properties. Venn diagrams were drawn using MetaCoMET (76) to visualize the unique OTUs in iDNA and eDNA fractions and the OTUs shared by the two DNA fractions.

Shotgun metagenomic sequencing and bioinformatics analyses. The library for shotgun metagenomic sequencing was prepared using a transposase-based method with the Nextera DNA Library Prep kit (Illumina). Given the extremely low DNA yield in the older sediments, the procedures for library preparation were optimized by extending the cycles of PCR to 16 in order to obtain sufficient amplified DNA for sequencing. A total of five metagenomes (1.4iDNA, 1.4eDNA, 11.8iDNA, 11.8eDNA, and 24.8iDNA), ~150 million short reads (150 bp, paired end) in total, were generated on the Illumina HiSeq 2500 system. Metagenomic sequencing was not possible for the 24.8eDNA fraction, because the trace amount of DNA resulted in the failure of library preparation. The raw sequences were first quality-filtered using the pipelines in Galaxy at Princeton University as described above. PhyloSift was used to infer the microbial community composition from the unassembled reads of the metagenome based on the phylogeny of a suite of single-copy marker genes in the standard PhyloSift database (77). The classification of the functional genes and their relative abundances (expressed as a percentage normalized to the total number of reads) were determined using GraftM and the packages published therein (78). In addition to the packages provided in GraftM (78), customized packages were constructed to analyze functional genes related to sporulation, O_2 respiration (cytochrome *c* oxidase), sulfate reduction, and the fermentation of peptides and amino acids.

Cell separation and enumeration by dual staining. In order to separate cells from ancient permafrost sediment, we adopted a previously published protocol using multiple density gradients of Nycodenz and sodium polytungstate (79). The sediment (5 g) was thawed and homogenized with a 20-ml solution of 1× phosphate-buffered saline (PBS) (pH 7.4) in 50-ml Falcon tubes. To increase the efficiency of cell detachment, 2.5 ml of detergent mix (50 mM EDTA, 100 mM sodium pyrophosphate, and 5% Tween 80) was added, and the mixture was shaken for 60 min at 500 rpm. The homogenized slurry was loaded onto a multiple density gradient consisting of sodium polytungstate (2.15 g/ml) and three layers of Nycodenz (1.42, 1.27, and 1.16 g/ml) as described previously (79). All samples were then centrifuged at 15,000 × *g* for 60 min at 4°C. The aqueous upper layers were collected and centrifuged at 12,000 × *g* for 10 min. The pellets were resuspended with 1.5 ml PBS solution and were centrifuged again at 12,000 × *g* for 10 min. The supernatant was discarded, and the cell pellets were resuspended in 1 ml PBS solution.

The LIVE/DEAD BacLight bacterial viability kit (Invitrogen, Carlsbad, CA) was used to enumerate the potential live and dead cells. The live cells with intact cell membranes would be stained green by the membrane-permeant dye (Syto9), whereas the red dye (propidium iodide [PI]) can penetrate only the membrane-compromised dead cells. Briefly, 50 μl of the cell suspension was mixed with 50 μl of the dye mixture to achieve a final concentration of 6 μM Syto9 or 30 μM PI. The samples were incubated in the dark for 15 min and were then filtered onto a 0.2-μm black polycarbonate membrane via a vacuum system. The live (green-fluorescing) and potentially dead (red-fluorescing) cells were visualized and imaged using epifluorescence microscopy (Olympus BX60; Olympus America Inc., Melville, NY).

Asp racemization assay by HPLC. The sediment (1 g) was mixed with 1.5 N HCl (1 ml) to remove carbonate as described previously (25). The demineralized sediment was first dried and then hydrolyzed by adding 10 ml 6 N HCl as described in a previous study (26). The hydrolysis was performed at 105°C for 16 h under N_2, and then the reaction was stopped on ice to cool down the reaction products. An aliquot of the hydrolysate (100 μl) was transferred to glass vials and was dried under a fume hood. The dried

residues were dissolved in 1 ml Milli-Q water and dried again in a speed vacuum concentrator. The final hydrolyzed products were dissolved in 4 ml Milli-Q water and stored at −20°C prior to analysis. To hydrolyze the separated cells, the cell suspension (0.5 ml) was centrifuged at 14,000 × *g* for 5 min, and then 6 N HCl (0.5 ml) was added to resuspend the pellet. The homogenized cell suspension was incubated at 105°C for 16 h under N_2 as described above. The hydrolysate (100 μl) was first dried and then dissolved in 1 ml Milli-Q water. To reduce interference in Asp detection, 5 to 10 μl NaOH (1 N) was added to each sample, and the sample was immediately centrifuged at 14,000 × *g* for 5 min to remove any soluble iron after precipitation. The supernatant was filtered (pore size, 0.2 μm) and stored at −20°C prior to high-performance liquid chromatography (HPLC) analysis.

To quantify D- and L-Asp acids in the hydrolysate, a modified HPLC procedure was adopted from a previous study (26). The amino acids were derivatized with *o*-phthaldialdehyde–*N*-acetyl-L-cysteine as described previously (27) and were immediately analyzed by HPLC. The HPLC was equipped with a PU-1580 pump (JASCO, Japan), a Nova-Pak C_{18} column (300 by 3.9 mm; particle size, 5 mm; Waters, USA), and an FP-1520 fluorescence detector (JASCO, Japan). D- and L-Asp acids were eluted with a binary mobile phase consisting of methanol and 50 mM sodium acetate buffer (pH 5.4). The flow rate was 0.6 ml/min, and the gradient conditions can be found in Table S1 in the supplemental material. Triplicate measurements were performed for all samples. Background racemization during hydrolysis at high temperatures was determined and was subtracted from the D-Asp/L-Asp values measured for the samples as suggested in a previous study (27). All glassware used during hydrolysis and other steps was treated with 4 N HCl and baked at 450°C overnight to remove any residual amino acid contamination. Blanks with no sediment were run in parallel, and no significant D- or L-Asp was detected in blanks compared with samples.

The racemization rate was calculated according to the Arrhenius equation:

$$k = Ae^{\left(\frac{-E_a}{RT}\right)} \quad (1)$$

in which k is the racemization rate constant, E_a is the activation energy (in kilijoules per mole), A is the frequency factor, R refers to the universal gas constant (8.314×10^{-3} kJ K^{-1} mol^{-1}), and T is temperature (on the kelvin scale). The kinetic parameters of Asp racemization in permafrost sediment (25) were used to extrapolate the specific racemization rate constant of each sample based on the *in situ* temperatures at corresponding depths (Table S2 in the supplemental material). We assumed that the temperature of the sediment had been stable under frozen conditions and predicted the D-Asp/L-Asp ratio for each depth using equation 2 below:

$$\ln_t\left[\frac{1+\mathrm{D/L}}{1-\mathrm{D/L}}\right] - ln_0\left[\frac{1+\mathrm{D/L}}{1-\mathrm{D/L}}\right] = 2kt \quad (2)$$

where D/L refers to the ratio of D-Asp to L-Asp and t is time.

Accession number(s). All raw sequence data obtained in this study were deposited in the NCBI Sequence Read Archive (SRA) under Bioproject number PRJNA505516 with accession numbers SRR8187969 and SRR8188252 to SRR8188256.

SUPPLEMENTAL MATERIAL

Supplemental material for this article may be found at https://doi.org/10.1128/AEM.00560-19.

SUPPLEMENTAL FILE 1, PDF file, 0.5 MB.

ACKNOWLEDGMENTS

This research was supported by NSF awards (DEB-1442059 and EAR-1528492) to T.O., NSF awards DEB-1442262 and 1460058 (Office Of International Science & Engineering) to T.V., and Russian Government Assignment grants AAAA-A18-118013190181-6 and PP ARCTICA AAAA-A18-118013190182-3 to E.M.R.

We declare that we have no conflicts of interest.

REFERENCES

1. Steven B, Léveillé R, Pollard WH, Whyte LG. 2006. Microbial ecology and biodiversity in permafrost. Extremophiles 10:259–267. https://doi.org/10.1007/s00792-006-0506-3.
2. Jansson JK, Taş N. 2014. The microbial ecology of permafrost. Nat Rev Microbiol 12:414. https://doi.org/10.1038/nrmicro3262.
3. Mackelprang R, Burkert A, Haw M, Mahendrarajah T, Conaway CH, Douglas TA, Waldrop MP. 2017. Microbial survival strategies in ancient permafrost: insights from metagenomics. ISME J 11:2305. https://doi.org/10.1038/ismej.2017.93.
4. Lau MCY, Stackhouse BT, Layton AC, Chauhan A, Vishnivetskaya TA, Chourey K, Ronholm J, Mykytczuk NCS, Bennett PC, Lamarche-Gagnon G, Burton N, Pollard WH, Omelon CR, Medvigy DM, Hettich RL, Pfiffner SM, Whyte LG, Onstott TC. 2015. An active atmospheric methane sink in high Arctic mineral cryosols. ISME J 9:1880. https://doi.org/10.1038/ismej.2015.13.
5. Chauhan A, Layton AC, Vishnivetskaya TA, Williams D, Pfiffner SM, Rekepalli B, Stackhouse B, Lau MC, Phelps TJ, Mykytczuk N. 2014. Metagenomes from thawing low-soil-organic-carbon mineral cryosols and permafrost of the Canadian high Arctic. Genome Announc 2:e01217-14. https://doi.org/10.1128/genomeA.01217-14.
6. Torti A, Lever MA, Jørgensen BB. 2015. Origin, dynamics, and implications of extracellular DNA pools in marine sediments. Mar Genomics 24:185–196. https://doi.org/10.1016/j.margen.2015.08.007.
7. Nagler M, Insam H, Pietramellara G, Ascher-Jenull J. 2018. Extracellular DNA in natural environments: features, relevance and applications. Appl Microbiol Biotechnol 102:6343–6356. https://doi.org/10.1007/s00253-018-9120-4.

8. Carini P, Marsden PJ, Leff JW, Morgan EE, Strickland MS, Fierer N. 2016. Relic DNA is abundant in soil and obscures estimates of soil microbial diversity. Nat Microbiol 2:16242. https://doi.org/10.1038/nmicrobiol.2016.242.
9. Torti A, Jørgensen BB, Lever MA. 2018. Preservation of microbial DNA in marine sediments: insights from extracellular DNA pools. Environ Microbiol 20:4526–4542. https://doi.org/10.1111/1462-2920.14401.
10. Willerslev E, Hansen AJ, Rønn R, Brand TB, Barnes I, Wiuf C, Gilichinsky D, Mitchell D, Cooper A. 2004. Long-term persistence of bacterial DNA. Curr Biol 14:R9–R10. https://doi.org/10.1016/j.cub.2003.12.012.
11. Vorobyova E, Soina V, Mulukin A. 1996. Microorganisms and enzyme activity in permafrost after removal of long-term cold stress. Adv Space Res 18:103–108. https://doi.org/10.1016/0273-1177(96)00005-1.
12. Mulyukin AL, Soina VS, Demkina EV, Kozlova AN, Suzina NE, Dmitriev VV, Duda VI, El'-Registan GI. 2003. Formation of resting cells by non-spore-forming microorganisms as a strategy of long-term survival in the environment, Proc SPIE 4939:208–219. https://doi.org/10.1117/12.486686.
13. Johnson SS, Hebsgaard MB, Christensen TR, Mastepanov M, Nielsen R, Munch K, Brand T, Gilbert MTP, Zuber MT, Bunce M, Rønn R, Gilichinsky D, Froese D, Willerslev E. 2007. Ancient bacteria show evidence of DNA repair. Proc Natl Acad Sci U S A 104:14401–14405. https://doi.org/10.1073/pnas.0706787104.
14. Lewis K, Epstein S, Godoy VG, Hong S-H. 2008. Intact DNA in ancient permafrost. Trends Microbiol 16:92–94. https://doi.org/10.1016/j.tim.2008.01.002.
15. Kryazhevskikh NA, Demkina EV, Manucharova NA, Soina VS, Gal'chenko VF, El'-Registan GI. 2012. Reactivation of dormant and nonculturable bacterial forms from paleosoils and subsoil permafrost. Microbiology 81:435–445. https://doi.org/10.1134/S0026261712040108.
16. Bakermans C, Tsapin AI, Souza-Egipsy V, Gilichinsky DA, Nealson KH. 2003. Reproduction and metabolism at −10°C of bacteria isolated from Siberian permafrost. Environ Microbiol 5:321–326. https://doi.org/10.1046/j.1462-2920.2003.00419.x.
17. Shi T, Reeves R, Gilichinsky D, Friedmann E. 1997. Characterization of viable bacteria from Siberian permafrost by 16S rDNA sequencing. Microb Ecol 33:169–179. https://doi.org/10.1007/s002489900019.
18. Vishnivetskaya TA, Petrova MA, Urbance J, Ponder M, Moyer CL, Gilichinsky DA, Tiedje JM. 2006. Bacterial community in ancient Siberian permafrost as characterized by culture and culture-independent methods. Astrobiology 6:400–414. https://doi.org/10.1089/ast.2006.6.400.
19. Vatsurina A, Badrutdinova D, Schumann P, Spring S, Vainshtein M. 2008. *Desulfosporosinus hippei* sp. nov., a mesophilic sulfate-reducing bacterium isolated from permafrost. Int J Syst Evol Microbiol 58:1228–1232. https://doi.org/10.1099/ijs.0.65368-0.
20. Steven B, Briggs G, McKay CP, Pollard WH, Greer CW, Whyte LG. 2007. Characterization of the microbial diversity in a permafrost sample from the Canadian high Arctic using culture-dependent and culture-independent methods. FEMS Microbiol Ecol 59:513–523. https://doi.org/10.1111/j.1574-6941.2006.00247.x.
21. Hansen AA, Herbert RA, Mikkelsen K, Jensen LL, Kristoffersen T, Tiedje JM, Lomstein BA, Finster KW. 2007. Viability, diversity and composition of the bacterial community in a high Arctic permafrost soil from Spitsbergen, Northern Norway. Environ Microbiol 9:2870–2884. https://doi.org/10.1111/j.1462-2920.2007.01403.x.
22. Setlow P. 1994. Mechanisms which contribute to the long-term survival of spores of *Bacillus* species. J Appl Bacteriol 76:49S–60S. https://doi.org/10.1111/j.1365-2672.1994.tb04357.x.
23. Amato P, Doyle SM, Battista JR, Christner BC. 2010. Implications of subzero metabolic activity on long-term microbial survival in terrestrial and extraterrestrial permafrost. Astrobiology 10:789–798. https://doi.org/10.1089/ast.2010.0477.
24. Dieser M, Battista JR, Christner BC. 2013. Double-strand DNA break repair at −15°C. Appl Environ Microbiol 79:7662–7668. https://doi.org/10.1128/AEM.02845-13.
25. Brinton KL, Tsapin AI, Gilichinsky D, McDonald GD. 2002. Aspartic acid racemization and age-depth relationships for organic carbon in Siberian permafrost. Astrobiology 2:77–82. https://doi.org/10.1089/153110702753621358.
26. Langerhuus AT, Røy H, Lever MA, Morono Y, Inagaki F, Jørgensen BB, Lomstein BA. 2012. Endospore abundance and D:L-amino acid modeling of bacterial turnover in Holocene marine sediment (Aarhus Bay). Geochim Cosmochim Acta 99:87–99. https://doi.org/10.1016/j.gca.2012.09.023.
27. Onstott TC, Magnabosco C, Aubrey AD, Burton AS, Dworkin JP, Elsila JE, Grunsfeld S, Cao BH, Hein JE, Glavin DP, Kieft TL, Silver BJ, Phelps TJ, van Heerden E, Opperman DJ, Bada JL. 2014. Does aspartic acid racemization constrain the depth limit of the subsurface biosphere? Geobiology 12:1–19. https://doi.org/10.1111/gbi.12069.
28. Braun S, Mhatre SS, Jaussi M, Røy H, Kjeldsen KU, Pearce C, Seidenkrantz M-S, Jørgensen BB, Lomstein BA. 2017. Microbial turnover times in the deep seabed studied by amino acid racemization modelling. Sci Rep 7:5680. https://doi.org/10.1038/s41598-017-05972-z.
29. Lomstein BA, Langerhuus AT, D'Hondt S, Jørgensen BB, Spivack AJ. 2012. Endospore abundance, microbial growth and necromass turnover in deep sub-seafloor sediment. Nature 484:101–104. https://doi.org/10.1038/nature10905.
30. Møller MH, Glombitza C, Lever MA, Deng L, Morono Y, Inagaki F, Doll M, Su C-C, Lomstein BA. 2018. D:L-Amino acid modeling reveals fast microbial turnover of days to months in the subsurface hydrothermal sediment of Guaymas Basin. Front Microbiol 9:967. https://doi.org/10.3389/fmicb.2018.00967.
31. Tsapin AI, McDonald G. 2003. Microorganisms buried in permafrost—are they in a dormant state or is their metabolism slowed down? p 1141–1144. *In* Phillips M, Springman SM, Arenson LU (ed), Permafrost: Proceedings of the Eighth International Conference on Permafrost, 21–25 July 2003, Zurich, Switzerland, vol 2. Balkema, Lisse, Netherlands.
32. Rivkina E, Gilichinsky D, Wagener S, Tiedje J, McGrath J. 1998. Biogeochemical activity of anaerobic microorganisms from buried permafrost sediments. Geomicrobiol J 15:187–193. https://doi.org/10.1080/01490459809378075.
33. Rivkina E, Shcherbakova V, Laurinavichius K, Petrovskaya L, Krivushin K, Kraev G, Pecheritsina S, Gilichinsky D. 2007. Biogeochemistry of methane and methanogenic archaea in permafrost. FEMS Microbiol Ecol 61:1–15. https://doi.org/10.1111/j.1574-6941.2007.00315.x.
34. Rivkina E, Laurinavichius K, McGrath J, Tiedje J, Shcherbakova V, Gilichinsky D. 2004. Microbial life in permafrost. Adv Space Res 33:1215–1221. https://doi.org/10.1016/j.asr.2003.06.024.
35. Rivkina E, Petrovskaya L, Vishnivetskaya T, Krivushin K, Shmakova L, Tutukina M, Meyers A, Kondrashov F. 2016. Metagenomic analyses of the late Pleistocene permafrost—additional tools for reconstruction of environmental conditions. Biogeosciences 13:2207–2219. https://doi.org/10.5194/bg-13-2207-2016.
36. Lomstein BA, Jørgensen BB, Schubert CJ, Niggemann J. 2006. Amino acid biogeo- and stereochemistry in coastal Chilean sediments. Geochim Cosmochim Acta 70:2970–2989. https://doi.org/10.1016/j.gca.2006.03.015.
37. Steen AD, Jørgensen BB, Lomstein BA. 2013. Abiotic racemization kinetics of amino acids in marine sediments. PLoS One 8:e71648. https://doi.org/10.1371/journal.pone.0071648.
38. Haglund A-L, Lantz P, Törnblom E, Tranvik L. 2003. Depth distribution of active bacteria and bacterial activity in lake sediment. FEMS Microbiol Ecol 46:31–38. https://doi.org/10.1016/S0168-6496(03)00190-9.
39. Kallmeyer J, Grewe S, Glombitza C, Kitte JA. 2015. Microbial abundance in lacustrine sediments: a case study from Lake Van, Turkey. Int J Earth Sci (Geol Rundsch) 104:1667–1677. https://doi.org/10.1007/s00531-015-1219-6.
40. Luna G, Manini E, Danovaro R. 2002. Large fraction of dead and inactive bacteria in coastal marine sediments: comparison of protocols for determination and ecological significance. Appl Environ Microbiol 68:3509–3513. https://doi.org/10.1128/aem.68.7.3509-3513.2002.
41. Braun S, Morono Y, Becker KW, Hinrichs K-U, Kjeldsen KU, Jørgensen BB, Lomstein BA. 2016. Cellular content of biomolecules in sub-seafloor microbial communities. Geochim Cosmochim Acta 188:330–351. https://doi.org/10.1016/j.gca.2016.06.019.
42. Salter SJ, Cox MJ, Turek EM, Calus ST, Cookson WO, Moffatt MF, Turner P, Parkhill J, Loman NJ, Walker AW. 2014. Reagent and laboratory contamination can critically impact sequence-based microbiome analyses. BMC Biol 12:87. https://doi.org/10.1186/s12915-014-0087-z.
43. Schulze-Makuch D, Wagner D, Kounaves SP, Mangelsdorf K, Devine KG, de Vera J-P, Schmitt-Kopplin P, Grossart H-P, Parro V, Kaupenjohann M, Galy A, Schneider B, Airo A, Frösler J, Davila AF, Arens FL, Cáceres L, Cornejo FS, Carrizo D, Dartnell L, DiRuggiero J, Flury M, Ganzert L, Gessner MO, Grathwohl P, Guan L, Heinz J, Hess M, Keppler F, Maus D, McKay CP, Meckenstock RU, Montgomery W, Oberlin EA, Probst AJ, Sáenz JS, Sattler T, Schirmack J, Sephton MA, Schloter M, Uhl J, Valenzuela B, Vestergaard G, Wörmer L, Zamorano P. 2018. Transitory microbial habitat in the hyperarid Atacama Desert. Proc Natl Acad Sci U S A 115:2670–2675. https://doi.org/10.1073/pnas.1714341115.
44. Levy-Booth DJ, Campbell RG, Gulden RH, Hart MM, Powell JR, Klironomos JN, Pauls KP, Swanton CJ, Trevors JT, Dunfield KE. 2007. Cycling

of extracellular DNA in the soil environment. Soil Biol Biochem 39:2977–2991. https://doi.org/10.1016/j.soilbio.2007.06.020.
45. Vonk JE, Mann PJ, Davydov S, Davydova A, Spencer RGM, Schade J, Sobczak WV, Zimov N, Zimov S, Bulygina E, Eglinton TI, Holmes RM. 2013. High biolability of ancient permafrost carbon upon thaw. Geophys Res Lett 40:2689–2693. https://doi.org/10.1002/grl.50348.
46. Onyenwoke RU, Brill JA, Farahi K, Wiegel J. 2004. Sporulation genes in members of the low G+C Gram-type-positive phylogenetic branch (*Firmicutes*). Arch Microbiol 182:182–192.
47. Brown DP, Ganova-Raeva L, Green BD, Wilkinson SR, Young M, Youngman P. 1994. Characterization of *spo0A* homologues in diverse *Bacillus* and *Clostridium* species identifies a probable DNA-binding domain. Mol Microbiol 14:411–426. https://doi.org/10.1111/j.1365-2958.1994.tb02176.x.
48. Donnelly ML, Fimlaid KA, Shen A. 2016. Characterization of *Clostridium difficile* spores lacking either SpoVAC or DPA synthetase. J Bacteriol 198:1694–1707. https://doi.org/10.1128/JB.00986-15.
49. Setlow P. 2007. I will survive: DNA protection in bacterial spores. Trends Microbiol 15:172–180. https://doi.org/10.1016/j.tim.2007.02.004.
50. Xue Y, Nicholson WL. 1996. The two major spore DNA repair pathways, nucleotide excision repair and spore photoproduct lyase, are sufficient for the resistance of *Bacillus subtilis* spores to artificial UV-C and UV-B but not to solar radiation. Appl Environ Microbiol 62:2221–2227.
51. Cox MM. 1999. Recombinational DNA repair in bacteria and the RecA protein. Prog Nucleic Acids Res Mol Biol 63:311–366. https://doi.org/10.1016/S0079-6603(08)60726-6.
52. Hiom K. 2003. DNA repair: bacteria join in. Curr Biol 13:R28–R30. https://doi.org/10.1016/S0960-9822(02)01385-4.
53. Li C, Clarke S. 1992. A protein methyltransferase specific for altered aspartyl residues is important in *Escherichia coli* stationary-phase survival and heat-shock resistance. Proc Natl Acad Sci U S A 89:9885–9889. https://doi.org/10.1073/pnas.89.20.9885.
54. Li C, Clarke S. 1992. Distribution of an L-isoaspartyl protein methyltransferase in eubacteria. J Bacteriol 174:355–361. https://doi.org/10.1128/jb.174.2.355-361.1992.
55. Setlow P. 2006. Spores of *Bacillus subtilis*: their resistance to and killing by radiation, heat and chemicals. J Appl Microbiol 101:514–525. https://doi.org/10.1111/j.1365-2672.2005.02736.x.
56. Shmelev D, Veremeeva A, Kraev G, Kholodov A, Spencer RG, Walker WS, Rivkina E. 2017. Estimation and sensitivity of carbon storage in permafrost of North-Eastern Yakutia. Permafrost Periglac Processes 28:379–390. https://doi.org/10.1002/ppp.1933.
57. Rawlings ND, Barrett AJ, Bateman A. 2010. MEROPS: the peptidase database. Nucleic Acids Res 38:D227–D233. https://doi.org/10.1093/nar/gkp971.
58. Lloyd KG, Schreiber L, Petersen DG, Kjeldsen KU, Lever MA, Steen AD, Stepanauskas R, Richter M, Kleindienst S, Lenk S, Schramm A, Jørgensen BB. 2013. Predominant archaea in marine sediments degrade detrital proteins. Nature 496:215–218. https://doi.org/10.1038/nature12033.
59. Hall D, Cammack R, Rao K. 1971. Role for ferredoxins in the origin of life and biological evolution. Nature 233:136–138. https://doi.org/10.1038/233136a0.
60. Fonknechten N, Chaussonnerie S, Tricot S, Lajus A, Andreesen JR, Perchat N, Pelletier E, Gouyvenoux M, Barbe V, Salanoubat M, Le Paslier D, Weissenbach J, Cohen GN, Kreimeyer A. 2010. *Clostridium sticklandii*, a specialist in amino acid degradation: revisiting its metabolism through its genome sequence. BMC Genomics 11:555. https://doi.org/10.1186/1471-2164-11-555.
61. Pester M, Brambilla E, Alazard D, Rattei T, Weinmaier T, Han J, Lucas S, Lapidus A, Cheng J-F, Goodwin L, Pitluck S, Peters L, Ovchinnikova G, Teshima H, Detter JC, Han CS, Tapia R, Land ML, Hauser L, Kyrpides NC, Ivanova NN, Pagani I, Huntmann M, Wei C-L, Davenport KW, Daligault H, Chain PSG, Chen A, Mavromatis K, Markowitz V, Szeto E, Mikhailova N, Pati A, Wagner M, Woyke T, Ollivier B, Klenk H-P, Spring S, Loy A. 2012. Complete genome sequences of *Desulfosporosinus orientis* DSM765^T, *Desulfosporosinus youngiae* DSM17734^T, *Desulfosporosinus meridiei* DSM13257^T, and *Desulfosporosinus acidiphilus* DSM22704^T. J Bacteriol 194:6300–6301. https://doi.org/10.1128/JB.01392-12.
62. Hausmann B, Pelikan C, Rattei T, Loy A, Pester M. 2019. Long-term transcriptional activity at zero growth of a cosmopolitan rare biosphere member. mBio 10:e02189-18. https://doi.org/10.1128/mBio.02189-18.
63. de Bok FA, Stams AJ, Dijkema C, Boone DR. 2001. Pathway of propionate oxidation by a syntrophic culture of *Smithella propionica* and *Methanospirillum hungatei*. Appl Environ Microbiol 67:1800–1804. https://doi.org/10.1128/AEM.67.4.1800-1804.2001.
64. Sieber JR, Sims DR, Han C, Kim E, Lykidis A, Lapidus AL, McDonnald E, Rohlin L, Culley DE, Gunsalus R, McInerney MJ. 2010. The genome of *Syntrophomonas wolfei*: new insights into syntrophic metabolism and biohydrogen production. Environ Microbiol 12:2289–2301. https://doi.org/10.1111/j.1462-2920.2010.02237.x.
65. Yamamoto K, Tamaki H, Cadillo-Quiroz H, Imachi H, Kyrpides N, Woyke T, Goodwin L, Zinder SH, Kamagata Y, Liu W-T. 2014. Complete genome sequence of *Methanoregula formicica* SMSP^T, a mesophilic hydrogenotrophic methanogen isolated from a methanogenic upflow anaerobic sludge blanket reactor. Genome Announc 2:e00870-14. https://doi.org/10.1128/genomeA.00870-14.
66. Bräuer S, Cadillo-Quiroz H, Kyrpides N, Woyke T, Goodwin L, Detter C, Podell S, Yavitt JB, Zinder SH. 2015. Genome of *Methanoregula boonei* 6A8 reveals adaptations to oligotrophic peatland environments. Microbiology 161:1572–1581. https://doi.org/10.1099/mic.0.000117.
67. Kraev G, Rivkina E, Vishnivetskaya T, Belonosov A, van Huissteden J, Kholodov A, Smirnov A, Kudryavtsev A, Teshebaeva K, Zamolodchikov D. 2019. Methane in gas shows from boreholes in epigenetic permafrost of Siberian Arctic. Geosciences 9:67. https://doi.org/10.3390/geosciences9020067.
68. Lennon J, Muscarella M, Placella S, Lehmkuhl B. 2018. How, when, and where relic DNA affects microbial diversity. mBio 9:e00637-18. https://doi.org/10.1128/mBio.00637-18.
69. Starnawski P, Bataillon T, Ettema TJG, Jochum LM, Schreiber L, Chen X, Lever MA, Polz MF, Jørgensen BB, Schramm A, Kjeldsen KU. 2017. Microbial community assembly and evolution in subseafloor sediment. Proc Natl Acad Sci U S A 114:2940–2945. https://doi.org/10.1073/pnas.1614190114.
70. Rivkina E, Abramov A, Spirina E, Petrovskaya L, Shatilovich A, Shmakova L, Scherbakova V, Vishnivetskaya T. 2018. Earth's perennially frozen environments as a model of cryogenic planet ecosystems. Permafrost Periglac Processes 29:246–256. https://doi.org/10.1002/ppp.1987.
71. Taberlet P, Prud'Homme SM, Campione E, Roy J, Miquel C, Shehzad W, Gielly L, Rioux D, Choler P, Clément J-C, Melodelima C, Pompanon F, Coissac E. 2012. Soil sampling and isolation of extracellular DNA from large amount of starting material suitable for metabarcoding studies. Mol Ecol 21:1816–1820. https://doi.org/10.1111/j.1365-294X.2011.05317.x.
72. Caporaso JG, Lauber CL, Walters WA, Berg-Lyons D, Huntley J, Fierer N, Owens SM, Betley J, Fraser L, Bauer M, Gormley N, Gilbert JA, Smith G, Knight R. 2012. Ultra-high-throughput microbial community analysis on the Illumina HiSeq and MiSeq platforms. ISME J 6:1621. https://doi.org/10.1038/ismej.2012.8.
73. Caporaso JG, Kuczynski J, Stombaugh J, Bittinger K, Bushman FD, Costello EK, Fierer N, Peña AG, Goodrich JK, Gordon JI, Huttley GA, Kelley ST, Knights D, Koenig JE, Ley RE, Lozupone CA, McDonald D, Muegge BD, Pirrung M, Reeder J, Sevinsky JR, Turnbaugh PJ, Walters WA, Widmann J, Yatsunenko T, Zaneveld J, Knight R. 2010. QIIME allows analysis of high-throughput community sequencing data. Nat Methods 7:335. https://doi.org/10.1038/nmeth.f.303.
74. Quast C, Pruesse E, Yilmaz P, Gerken J, Schweer T, Yarza P, Peplies J, Glöckner FO. 2012. The SILVA ribosomal RNA gene database project: improved data processing and web-based tools. Nucleic Acids Res 41:D590–D596. https://doi.org/10.1093/nar/gks1219.
75. Dhariwal A, Chong J, Habib S, King IL, Agellon LB, Xia J. 2017. MicrobiomeAnalyst: a web-based tool for comprehensive statistical, visual and meta-analysis of microbiome data. Nucleic Acids Res 45:W180–W188. https://doi.org/10.1093/nar/gkx295.
76. Wang Y, Xu L, Gu YQ, Coleman-Derr D. 2016. MetaCoMET: a web platform for discovery and visualization of the core microbiome. Bioinformatics 32:3469–3470. https://doi.org/10.1093/bioinformatics/btw507.
77. Darling AE, Jospin G, Lowe E, Matsen IF, Bik HM, Eisen JA. 2014. PhyloSift: phylogenetic analysis of genomes and metagenomes. PeerJ 2:e243. https://doi.org/10.7717/peerj.243.
78. Boyd JA, Woodcroft BJ, Tyson GW. 2018. GraftM: a tool for scalable, phylogenetically informed classification of genes within metagenomes. Nucleic Acids Res 46:e59. https://doi.org/10.1093/nar/gky174.
79. Morono Y, Terada T, Kallmeyer J, Inagaki F. 2013. An improved cell separation technique for marine subsurface sediments: applications for high-throughput analysis using flow cytometry and cell sorting. Environ Microbiol 15:2841–2849. https://doi.org/10.1111/1462-2920.12153.